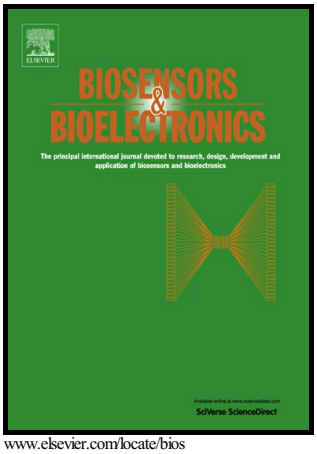

www.elsevier.com/locate/bios

A label-free and enzyme-free ultra-sensitive transcription factors biosensor using DNA-templated copper nanoparticles as fluorescent indicator and hairpin DNA cascade reaction as signal amplifier

Liang Sha, Xiaojun Zhang, Guangfeng Wang

PII: S0956-5663(16)30266-4
DOI: http://dx.doi.org/10.1016/j.bios.2016.03.066
Reference: BIOS8577

To appear in: *Biosensors and Bioelectronic*

Received date: 12 February 2016
Revised date: 23 March 2016
Accepted date: 25 March 2016

Cite this article as: Liang Sha, Xiaojun Zhang and Guangfeng Wang, A label-free and enzyme-free ultra-sensitive transcription factors biosensor using DNA templated copper nanoparticles as fluorescent indicator and hairpin DNA cascade reaction as signal amplifier, *Biosensors and Bioelectronic* http://dx.doi.org/10.1016/j.bios.2016.03.066

A label-free and enzyme-free ultra-sensitive transcription factors biosensor using DNA-templated copper nanoparticles as fluorescent indicator and hairpin DNA cascade reaction as signal amplifier

Liang Sha[a], Xiaojun Zhang[a] and Guangfeng Wang[a,b*]

a Key Laboratory of Chem-Biosensing, Anhui province; Key Laboratory of Functional Molecular Solids, Anhui province; College of Chemistry and Materials Science, Center for Nano Science and Technology, Anhui Normal University, Wuhu 241000, PR China

b State Key Laboratory of Chemo/Biosensing and Chemometrics, Hunan University, Changsha 410082, PR China

Corresponding Author: Guangfeng Wang

E-mail: wangyuz@mail.ahnu.edu.cn

Fax: +86-553-3869303; Tel: +86-553-3869302

ABSTRACT: Detection and quantification of specific protein with ultralow concentration play a crucial role in biotechnological applications and biomedical diagnostics. In this paper, a label-free and enzyme-free amplified fluorescent biosensor has been developed for transcription factors detection based on AT-rich double-stranded DNA-templated copper nanoparticles (ds DNA/Cu NPs) and hairpin DNA cascade reaction. This strategy was demonstrated by using nuclear factor-kappa B p50 (NF-κB p50) and specific recognition sequences as a model case. In this assay, a triplex consists of double-stranded DNA containing NF-κB p50 specifically binding sequences and a special design single-stranded DNA (Trigger) which is able to activate the hairpin DNA cascade amplifier (HDCA). In the presence of NF-κB p50, the triplex became unstable since the target bound to the recognition sequences with strong affinity. The selective binding event confirmed that the Trigger was successfully released from the triplex and initiated HDCA to yield the product which could effectively template the formation of fluorescent Cu NPs. The experimental results revealed that the advanced strategy was ultra-sensitive for detecting NF-κB p50 in the concentration range from 0.1 to 1000 pM with a detection limit of 0.096 pM. In addition, the relative standard deviation was 4.08% in 3 repetitive assays of 500 pM NF-κB p50, which indicated that the reproducibility of this strategy was acceptable. Besides desirable sensitivity, the developed biosensor also showed high selectivity, cost-effective, and simplified operations. In addition, the proposed bio-

sensing platform is versatile. By conjugating with various specific recognition units, it could hold considerable potential to sensitive and selective detect various DNA-binding proteins and might find wide applications in biomedical fields.

Keywords: Label-free; Enzyme-free; AT-rich ds DNA/Cu NPs; Hairpin DNA cascade reaction; Fluorescence; NF-κB p50

1. Introduction

Transcription factors (TFs) are a type of sequence specific DNA-binding proteins which can recognize the nucleic acids (6-12 base pairs) within the gene regulatory region and generally function in combinatorial manners to regulate the transcription of target genes (Spitz et al., 2012). Regular transcription is of vital importance to normal cellular function of accurate embryonic development, probably attribute to the fact that TFs play pivotal roles in the pathways and networks of cellular regulation and the expression levels sensitively reflect cellular development or disease state. However, irregular transcription might lead to a variety of violent diseases such as cancer (Darnell et al., 2002), diabetes (Sanchez et al., 2009), congenital heart disease (Clark et al., 2006), autoimmune diseases (Eggert et al., 2004; Peng et al 2008), and developmental syndromes (Spitz et al., 2012). Therefore, TFs have been recognized as attractive markers for disease diagnosis and drug development and become potential targets in biomedical diagnosis and drug development. Since TFs are usually expressed at an extremely low concentration in biological cells (Pabo et al., 1992), highly sensitive assays for the detection of TFs are eagerly required (Altevogt et al., 2009; Tan et al., 2010).

Signal amplification of recognition methods are usually employed in the construction of sensitive biosensors. Over past several decades, quite a few DNA based amplification methods have been frequently utilized for improving detection sensitivity, such as polymerase chain reaction (PCR) (Saiki et al., 1988), ligase chain reaction (LCR) (Barany et al., 1991), rolling circle amplification (RCA) (Fire et al., 1995), hybridization chain reaction (HCR) (Dirks et al., 2004), and

strand displacement amplification (SDA) (Walker et al., 1992). Even though the sensitivity is enhanced by these techniques, most of these amplified methods either involve enzyme and expensive instruments, which may narrow the application scope and lead to the potential occurrence of false positive results caused by non-specific protein interfering, or require rigorous operations like heating or cooling processes which are generally laborious and time-consuming.

Hairpin DNA cascade amplifier (HDCA), an enzyme-free DNA amplification technique, has been proven to be increasingly valuable for quantitative analysis of various biological molecules, due to it is an isothermal and homogeneous signal generation strategy with high signals and low noise (Scheme S1A). During the reaction, a pair of DNA hairpins (HP1 and HP2) could be designed to be complementary to one another but kinetically hindered by caging their complementary regions within the hairpin stems. However, in the presence of a nucleic acid input (Trigger), the stem part of HP1 is opened through a toehold-mediated strand displacement reaction. The newly exposed single-stranded DNA (ss DNA) region within HP1 can then hybridize to HP2 through a secondary toehold-mediated DNA strand displacement. During the secondary strand displacement, Trigger will be displaced and available for catalyzing a next round of hybridization between HP1 and HP2, which is re-used until the supply of HP1 or HP2 is exhausted. Similar to the catalyst in a chemical reaction, the sequence of Trigger plays a catalytic role in HDCA. Since Pierce, Yin, and co-workers reported HDCA originally in 2008 (Yin et al., 2008), various techniques such as electrochemistry, fluorescence, and colorimetry have combined with HDCA for amplified detection of numerous analytes (Zhang et al., 2015b; Xu et al., 2015; Quan et al., 2015). Among them, considerable HDCA based fluorescent biosensors have been developed due to the good sensitivity, strong selectivity and convenient application, obvious signal and simply experimental procedure. For example, Wu used hairpin DNA cascade reaction to provide high fluorescent signal gain of mRNA imaging inside live cells (Wu et al., 2015). Guo designed a logic gate operation for ultra-sensitive fluorescent detection of target DNA and adenosine triphosphate (ATP) based on HDCA as well (Guo et al., 2015). Unfavourably, most of the HDCA based fluorescent biosensors are dependent on dye-labelled fluorophore and quencher, which limits their wide ap-

plications due to some intrinsic disadvantages. For one thing, many fluorescent dyes are highly toxic and contaminating, which may lead to the potential occurrence of false positive results by interfering the target and severe effects upon human health and the environment (McCann et al., 1975; McCann et al., 1976). For another, the design and synthesis of labelled fluorophore are complicated and the labelling process suffers from high price and time-consuming optimization. In order to solve this problem, several researchers have reported label-free fluorescence methods for the sensitive detection of NF-κB p50. They utilized intercalating dyes, for example, Sybr Green I (SG), which is known to exhibit high affinity towards duplex DNA (Li et al., 2015; Liu et al., 2012). However, the use of intercalating dyes may increase the rigidity of duplex, which could lead to the decrease of sensitivity by interfering the interactions between the target NF-κB p50 and recognition sequences. Furthermore, even if a few HDCA based fluorescent biosensors have been successfully developed, most of them are designed primarily for the detection of nucleic acids (DNA or microRNA) (Zhang et al., 2015b), and protein detection represents another challenge. Therefore, it is necessary and significant to develop a label-free, cost-effective, and environmental-friendly HDCA based fluorescent strategy for the TFs detection.

Over past a few decades, biomolecules templated fluorescent inorganic metal nanoparticles have obtained generous attention (Sapsford et al., 2013). Among these biomolecules, oligonucleotide represents particularly good template candidate due to the unique nanosized structure, excellent programmable properties, and rich functional groups including heterocyclic nitrogen atoms, amino groups, and phosphate groups, which can bind with specific metal ions and provide nucleation sites for metallic nanoparticles. Nucleic acid-templated fluorescent metal nanoparticles have been intensely investigated in the past decade, such as gold nanoclusters (Au NCs) (Kennedy et al., 2012; Teng et al., 2015), silver nanoclusters (Ag NCs) (Richards et al., 2008; Enkin et al., 2014), and copper nanoparticles (Cu NPs) (Rotaru et al., 2010; Qing et al., 2013a). These DNA templated inorganic nanoparticles have the potential to be a label-free fluorescent indicator with mild reaction conditions and high efficiencies due to the fact that DNA are usually involved in the whole reaction system and strongly correlated to the target analytes. Since copper is a significant and

essential micronutrient for almost living animals and plants, implying its hypotoxicity and good biocompatibility (Koval et al., 2006; Yin et al., 2009), Cu NPs in applications should be safer than other heavy-metal nanoparticles and quantum dots. Meanwhile, because of the quantum size effect, Cu NPs emit in an entire spectral region of 500-650 nm upon excitation with 340 nm UV light (Qing et al., 2014). The mega-Stokes shift is advantageous for the removal of interference from background signals of complex biological systems and interference from excitation light source (Song et al., 2015). Thus, it is desirable to use the AT-rich ds DNA/Cu NPs as a label-free fluorescent indicator for biosensors. Up to now, Cu NPs have been utilized to construct simple and effective fluorescent biosensors for many analytes detection such as heavy metal ions like copper ions (Qing et al., 2014), lead ions(Chen et al., 2012); small biomolecules like biothiols (Zhang et al., 2015a), streptavidin (Wang et al., 2015); or the nuclease and its inhibitors (Qing et al., 2013b). However, the application of Cu NPs for biological sensing is still at an incipient stage, so it is encouraging to exploit in further application.

Inspired by the essentiality of label-free and enzyme-free amplified fluorescent detection of TFs, the advantages of AT-rich ds DNA/Cu NPs and HDCA, herein, a label-free and enzyme-free AT-rich ds DNA/Cu NPs-based fluorescent biosensing platform with HDCA amplification was ingeniously developed for ultra-sensitive detection of TFs. As the proof-of-concept, nuclear factor-kappa B p50 (NF-κB p50) which is involved in the regulation of a large number of genes and closely related to some diseases already mentioned is chosen as a model to be investigated (Sen et al., 1986). Due to the label-free AT-rich ds DNA/Cu NPs as a fluorescent indicator and signal amplification of enzyme-free HDCA, the proposed biosensing platform exhibited high sensitivity toward NF-κB p50 with a detection limit as low as 0.096 pM, and excellent specificity toward NF-κB p50 versus other non-targeted proteins. It may further be extended for detection of various DNA-binding proteins only by replacing the recognition units, holding a great potential for early diagnosis in biomedical fields.

2. Experimental section

2.1. Chemicals

All HPLC-purified oligonucleotides were purchased from Sangon Biotechnology Co. Ltd (Shanghai, China) and their sequences are listed in Table S1. The purified recombinant NF-κB p50 protein was purchased from Cayman Chemical (Ann Arbor, MI, USA). The human thrombin, human immunoglobulin G (human IgG), human serum album (HSA) and bovine serum albumin (BSA) were purchased from Sangon Biotechnology Co. Ltd (Shanghai, China). 3-(N-Morpholino) propanesulfonic acid (MOPS), silver nitrate, copper sulfate, sodium nitrate, sodium ascorbate, magnesium nitrate and the other commercial chemicals used in this experiment were purchased from the Sinopharm Chemical Reagent Co. Ltd. (Shanghai, China). These chemicals were of analytical grade at least and used without further purification. All solutions were prepared with ultrapure water (≥18.2 MΩ cm). The MOPS buffer (10 mM MOPS, 150 mM $NaNO_3$ and 2 mM $Mg(NO_3)_2$, pH=8.0) was prepared in ultrapure water. All of the experiments without mention were carried out at room temperature.

2.2. Instruments

All fluorescence spectra and real-time scan were measured by LS-55 fluorescence spectrophotometer (PerkinElmer Company, USA) at room temperature and the detected solution of 200 μL was placed in a 0.1×1 cm^2 micro quartz cuvette with a total volume of 350 μL. Ultraviolet-visible (UV-vis) absorption spectrum and UV melting curves were measured on UV-3010 spectrophotometer (Hitachi, Japan). High-resolution transmission electron micrograph (HRTEM) observations for the morphological measurements of Cu NPs were obtained with a Tecnai G220S-TWIN transmission electron microscope (FEI). Centrifugation was performed using a HERMLEZ 36 HK apparatus (Wehingen, Germany). Fluorescence emission images were taken by a common digital camera (Shanghai, China). Ultrapure water was obtained through PSDK2-10-C (Beijing, China). All pH measurements were measured with a Model pHs-3c meter (Shanghai, China).

2.3. Formation of triplex DNA structure

Prior to use, all the oligonucleotides stock solutions (100 μM) were prepared in 10 mM MOPS buffer (150 mM $NaNO_3$ and 2 mM Mg $(NO_3)_2$, pH=8.0) and stored at 4 °C overnight. The working solution of 4 μM was obtained by diluting the stock solution with 10 mM MOPS buffer. The DNA solution was heated to 90 °C for 10 min to remove aggregates, and then cooled slowly to room temperature for future use. First, to obtain the ds DNA, the corresponding complementary ss DNA (DNA1 and DNA2) were mixed at the same molar ratios with the final concentration of 2 μM in 10 mM MOPS buffer. The mixture was heated at 95 °C for 5 min and then slowly cooled down to room temperature. Then 5 μL ds DNA (2 μM) was mixed with 2.5 μL DNA3 (Trigger, 4 μM) and 2.5 μL $AgNO_3$ (400 μM) for 30 min to form triplex DNA structure stably in 10 mM MOPS buffer under dark treatment.

2.4. Amplified detection of target NF-κB p50

For the detection of target, 1 μL purified recombinant NF-κB p50 (100 nM) was added to above system to incubate 20 min at 37 °C. The final volume was 50 μL. To avoid steric hindrance preventing the HDCA process, we added HP1and HP2 until the reaction of NF-κB p50 finished. Then, 25 μL HP1 (4 μM) and 25 μL HP2 (4 μM) were added into the above mixture with 100 μL final volume. To achieve high sensitivity, the above solution was incubated for 2 h at 37 °C in 10 mM MOPS buffer. Thirdly, Cu NPs were synthesized in a typical procedure, 50 μL sodium ascorbate (8 mM) was added into the above solution. After incubation of 10 min at room temperature, 50 μL $CuSO_4$ (800 μM) was introduced to the resulting solution and incubated for another 10 min. The final volume was 200 μL. The final concentrations were 50 nM of ds DNA (DNA1-DNA2), 50 nM of DNA3 (Trigger), 500 nM of HP1, 500 nM of HP2, 5 μM of $AgNO_3$, 2 mM of sodium ascorbate, 200 μM of $CuSO_4$ and 500 pM of purified recombinant NF-κB p50, respectively. Finally, the resulted solutions were characterized by fluorescence spectrophotometer and the excimer fluorescence was recorded.

2.5. Selectivity assay

To investigate the specificity of the proposed biosensor for the target NF-κB p50, 0.5 nM purified recombinant NF-κB p50 and 5 nM of BSA / HSA / IgG / Thrombin / Mixture (above all containing the target) were added into the buffer respectively. The experimental procedures were the same as the aforementioned detection of NF-κB p50 in 10 mM MOPS buffer (150 mM $NaNO_3$ and 2 mM Mg $(NO_3)_2$, pH=8.0).

2.6. Fluorescence measurement

All fluorescence measurements were carried out at LS-55 fluorescence spectrophotometer with excitation at 340 nm and emission at 588 nm for the AT-rich ds DNA/Cu NPs. When the samples were excited at 340 nm, the emission was scanned from 500 to 650 nm in steps of 0.5 nm; the excitation and emission slits of the spectrophotometer were both set at 10.0 nm; the scanning speed was 1200 nm min^{-1}.

2.7. Gel electrophoresis analysis

In the gel electrophoresis assay, DNA3 (300 nM) or Triplex (DNA1, DNA2, DNA3, 300 nM each) / NF-κB p50 (3 nM) complex was incubated with 3 μM each of HP1 and HP2 at 37°C overnight. Each prepared sample (10 μL) was put on 5% agarose gels which were prepared to separate the related substances. The electrophoresis was carried in 0.5 × TBE buffer (25 mM Tris, 25 mM Boric Acid, 1.0 mM EDTA, pH 7.9) at 120 V constant voltage for 1 hour. The ethidium bromide (EB) was used as an oligonucleotide dye and mixed with samples for 30 min. After EB staining, the gels were scanned using the Omega 16ic Gel imaging system (UL-TRA-LUM, USA).

2.8. NF-κB p50 detection in HeLa cell nuclear extracts

To evaluate the practicality of the proposed biosensor, HeLa nuclear extracts were collected as a real sample. First, HeLa cells were cultured in Dulbecco's modified Eagle's medium (DMEM; Invitrogen, USA) with 10% fetal bovine serum (FBS; Invitrogen, USA) and 50 U/mL of penicillin plus 50 μg/mL of streptomycin at 37 °C with 5% CO_2. The nuclear extracts were prepared using

the nuclear extract kit (ActiveMotif, Carlsbad, CA). The sample was stored at -4 °C for further use (Li et al., 2012). Then, five concentrations of NF-κB p50 (1, 5, 10, 50, and 100 pM) were detected in HeLa cell nuclear extracts after spiking with standard NF-κB p50 solutions. The experimental procedures were the same as the aforementioned detection of NF-κB p50 in clean MOPS buffer solution. The recovery in the spiked sample calculated to investigate the feasibility of the strategy in biological sample.

3. Results and discussion

3.1. Principle of AT-rich ds DNA/Cu NPs-based fluorescent biosensing platform for NF-κB p50 detection

The working principle of the designed AT-rich ds DNA/Cu NPs-based fluorescent biosensing platform for NF-κB p50 detection is illustrated in Scheme 1A. In Part 1, DNA1 and DNA2 were completely complementary to form ds DNA containing NF-κB p50 recognition sequences that partially overlapped the homo-pyrimidine strand with a dual functional ssDNA (DNA3, Trigger) to form triplex DNA structure by Hoogsteen bond containing C•G◦C and T•A◦T triads (• denoted as Hoogsteen bond, ◦ denoted as Watson-Crick bond) (step 1). During the formation of triplex DNA structure, Ag^+ can specifically recognize the C•G◦C triads to form AgC•G◦C. Therefore, with the aid of Ag^+, the stability of the triplex could be definitely enhanced (Ihara et al., 2009; Xiao et al., 2013). In the absence of the target NF-κB p50, Trigger adhered to the ds DNA cannot initiate the HDCA for signal amplification. However, the affinity of NF-κB p50 for the ds DNA containing the recognition sequences was much stronger than that of Trigger. As a consequence, in the presence of NF-κB p50, it could strongly conjugate with ds DNA. Then, the triplex is not stable anymore, resulting in the gradual liberation of Trigger which is available to activate HDCA in the next part (step 2). In Part 2 (we marked roman numerals with '*' region complementary to the corresponding unmarked during the reaction), a pair of unlabelled hairpin DNA probes was rationally designed for HDCA. In Hairpin1 (HP1), at the stem region, region II and III (green and red, respectively) could hybridize with region II* and III*, respectively, resulting in a stable hairpin configuration which has a loop of region IV (purple) and an extra tail of region I (blue). Simultaneously, in Hairpin2 (HP2), region IV (purple) could hybridize with region IV* at the stem region, resulting in a stable hairpin configuration, which also has a loop of region II* and III* (green and red, respectively) and an extra tail of region III (red) in an initially locked format. The hairpin DNA probes (HP1 and HP2) can potentially hybridize to form a HP1-HP2 duplex with the catalysis of the free Trigger, since HP1 contains a segment that is complementary to a segment of HP2. However, in the absence of the Trigger, the spontaneous hybridization of the two hairpins is

kinetically hindered by complementary regions within intramolecular hairpin secondary structures (Tang et al., 2015). While as the Trigger released from the triplex, it would hybridize with the exposed toehold region I of HP1 which gradually initiates a strand displacement, generating a HP1-Trigger intermediate through region hybridization (I-II-III and III*-II*-I*) (step 3). The released toehold region IV in the HP1-Trigger intermediate further initiates branch migration (Li et al., 2011) on region III-IV*-III*-II* of HP2 (step 4), followed by displacement of Trigger, which, instead of being consumed, is released to catalyze the formation of other HP1-HP2 duplexes for the next catalytic round driven by system thermodynamic enthalpy decrease (Wu et al., 2015). Thus, the Trigger released by the target NF-κB p50 can initiate the hybridization between hairpin HP1 and HP2 for multiple cycles until the supply of HP1 or HP2 is exhausted. Due to the ingenious design of the hairpin probes, region III and III* (red) in HP1 and HP2 are the AT-rich single-stranded DNA sequence which could be the dominant template for the formation of highly fluorescent AT-rich ds DNA/Cu NPs when region III and III* are complementary to each other in HP1-HP2 duplex (Qing et al., 2014; Song et al., 2015). However, AT-rich sequence (region III and III*) is partially caged in the hairpin structure of the stem in HP1 (the tension from the loop of HP1) and the loop in HP2. Consequently, the dominant template is prohibited to effectively form the AT-rich ds DNA/Cu NPs. While after the achievement of HDCA, the duplexes could be dominant templates for the Cu NPs. As shown in Part 3, with the addition of sodium ascorbate and copper ions, AT-rich ds DNA/Cu NPs formed efficiently (step 5). By following the mechanism, one copy of target NF-κB p50 can open multiple hairpin probes to trigger numerous recycle reactions, which results in the generation of AT-rich ds DNA sequences producing massive ds DNA/Cu NPs as effective fluorescent indicator for label-free, enzyme-free biosensor based on hairpin DNA cascade reaction.

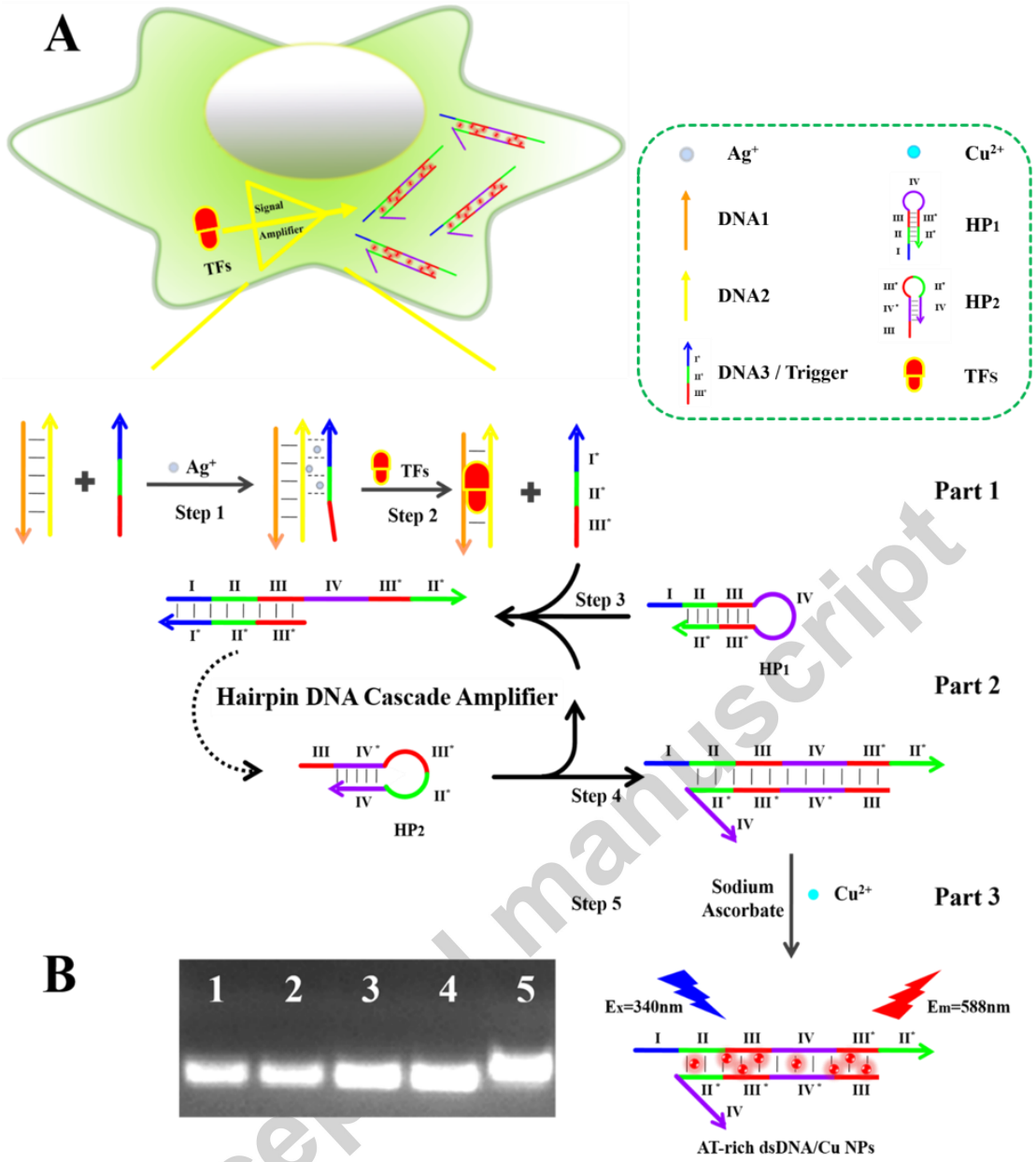

Scheme 1. (A) Schematic illustration of AT-rich ds DNA/Cu NPs as a fluorescent indicator for ultrasensitive detection of NF-κB p50 based on hairpin DNA cascade amplifier (HDCA). Roman numerals marked with * regions are complementary to the corresponding unmarked. (B) The gel electrophoresis images for the whole work principle: (1) 3 μM HP1; (2) 3 μM HP2; (3) 3 μM HP1 + 3 μM HP2; (4) 3 μM HP1 + 3 μM HP2 + 0.3 μM Triplex; (5) 3 μM HP1 + 3 μM HP2 + 0.3 μM Triplex + 3 nM NF-κB p50.

3.2. HRTEM, fluorescence spectrum, ultraviolet-visible (UV-vis) absorption spectrum and gel-electrophoresis characterization

Due to the proposed fluorescent biosensing platform for amplified NF-κB p50 detection is based on the indicator of AT-rich ds DNA/Cu NPs, the successful preparation of Cu NPs is the key through the whole system. Firstly, the prepared Cu NPs were characterized by HRTEM. As shown in Figure 1A, the copper nanoparticles are individually spherical and uniform. The particle size distribution given in Figure 1B shows that particles with varying size from 3 nm to 6 nm with a maximum around 4~5 nm. Moreover, AT-rich ds DNA/Cu NPs were characterized by fluorescence spectrum and UV-vis absorption spectrum and the results were shown in Figure 1C and Figure 1D, respectively. The maximum excitation and emission wavelengths of Cu NPs are 340 nm and 588 nm, respectively (curve a, curve b of Figure 1C). In the UV–vis spectrum (Figure 1D), the characteristic absorption peak of Cu NPs appears at approximately 340 nm which is similar to their excitation spectrum. The results verify that AT-rich ds DNA/Cu NPs have been successfully formed.

Gel electrophoresis assay was utilized to prove the whole work principle. As shown in Scheme 1B, it can be observed that in the absence of target NF-κB p50, there is only one band in lane 1, lane 2, lane 3 and lane 4, indicating that the cross-interaction between HP1 and HP2 is effectively blocked and no HDCA occurs. In the presence of NF-κB p50, the primary band disappears and an obvious new band emerges in lane 5, which indicates that the triplex destabilized by NF-κB p50 and effectively releases the Trigger to activate the HDCA reaction to form the HP1-HP2 duplexes.

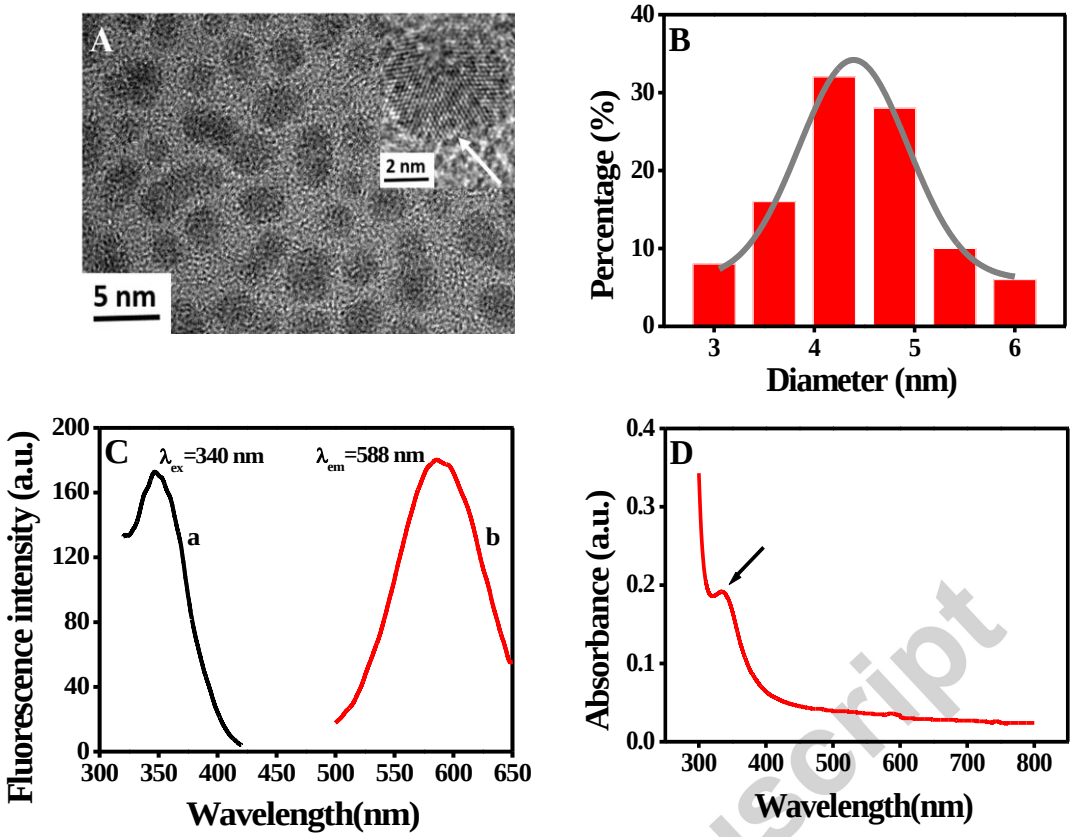

Figure 1. (A) HRTEM image of the synthetic AT-rich ds DNA/Cu NPs. The inset shows the crystal lattice structure of Cu NPs. (B) Size distribution analysis of AT-rich ds DNA/Cu NPs. (C) Fluorescence spectrum of AT-rich ds DNA/Cu NPs: (a) Fluorescence excitation (λ_{ex}= 340 nm) and (b) emission (λ_{em}= 588 nm). (D) UV–vis absorption spectrum of AT-rich ds DNA/Cu NPs. The arrow marks the characteristic absorption peak of Cu NPs (340 nm).

3.3. Feasibility of AT-rich ds DNA/Cu NPs-based fluorescent biosensing platform for NF-κB p50 detection

In order to confirm whether the fluorescence change of Cu NPs relied on the concentration of the Trigger, different concentrations of Trigger were investigated. As we can see from Figure S3A, with the concentration increases, the fluorescent intensity of Cu NPs enlarges. The linear relationship between the fluorescence peak changed at 588 nm and Trigger concentrations is achieved as well (Figure S3B, ESI†). In order to relate the NF-κB p50 concentration to the Trigger, we ingeniously design the triplex DNA structure which contains NF-κB p50 recognition sequences. After target NF-κB p50 combines with the recognition sequences, the triplex has been not stable any-

more, leading to the liberation of the Trigger which is available to activate HDCA to generate fluorescent signal.

To evaluate the feasibility of the designed fluorescence biosensing platform, the fluorescence signals upon the target NF-κB p50 in a series of control experiments were depicted in Figure 2A. The results indicate that HP1, HP2 and the triplex DNA individually (curve a, b, c of Figure 2A, respectively) or mixture (curve d of Figure 2A) could not form the fluorescent ds DNA/Cu NPs. As curve e of Figure 2A shows, in the presence of target NF-κB p50 into the mixture, a significant increase of fluorescent intensity can be observed which might contribute to the specific recognition of NF-κB p50 to the ds DNA sequences, producing the free Trigger for HDCA to generate the AT-rich templates for Cu NPs, causing an obvious fluorescent signal enhancement. Therefore, the current fluorescent biosensing platform is hopeful to offer a high feasibility for the detection of target NF-κB p50. The corresponding fluorescent emission images with UV-light excitation are also consistent with the above results (inset in Figure 2A).

Morkhir and co-workers reported that AT-rich ds DNA/Cu NPs might be formed in following steps: the reaction of reducing Cu^{2+} to Cu^{+} followed by the disproportionation of Cu^{+} into Cu^{2+} and Cu^{0} and aggregating of the latter on AT-rich ds DNA sequences, producing stable copper nanoparticles (Monson et al., 2003; Chen et al., 2015). To further explore the feasibility of the proposed strategy in constructing AT-rich ds DNA/Cu NPs biosensing platform, control experiments were carried out under the same experimental conditions. In this assay, random, GC-rich and AT-rich ds DNA sequences with the same amount of base pairs were tested as templates for Cu NPs formation. As shown in Figure 2B, it reveals that only AT-rich ds DNA sequences exhibit high fluorescence response. Meanwhile, by using random or GC-rich ds DNA as templates, little fluorescent signal can be observed, which demonstrate that only AT-rich ds DNA sequences would be used as dominant templates for the formation of fluorescent Cu NPs. The corresponding fluorescence emission images with UV-light excitation are also consistent with the above results (inset in Figure 2B).

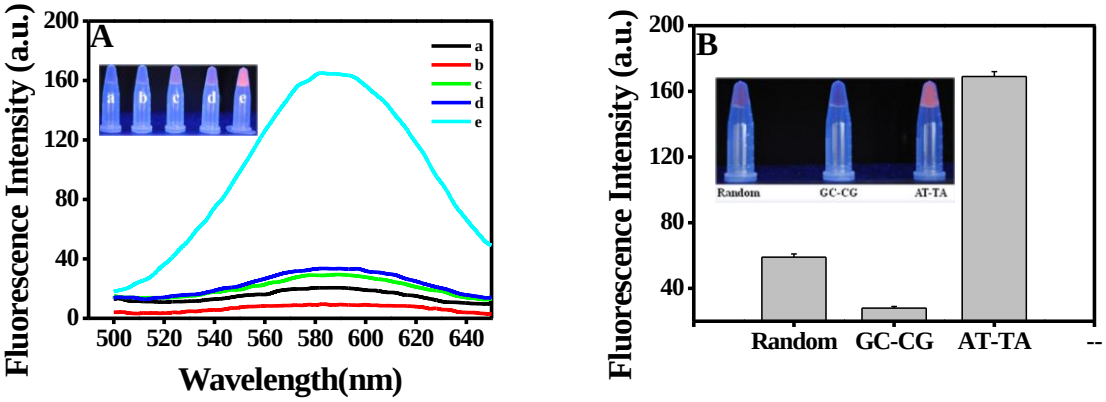

Figure 2. (A) Fluorescence response of the biosensing system under different conditions: (a) HP1, (b) HP2, (c) HP1+HP2, (d) HP1+HP2+Triplex, and (e) HP1+HP2+Triplex+NF-κB p50. (B) Fluorescence response of Cu NPs templated by different kinds of ds DNA (random, GC-rich, AT-rich ds DNA). The inset shows the corresponding fluorescent emission images with UV-light excitation. The error bars were the standard deviation of three repetitive measurements.

3.4. Analytical performance of AT-rich ds DNA/Cu NPs-based fluorescent biosensing platform for NF-κB p50 detection

Under the optimized experimental conditions (in supplemental information), the analytical performance of AT-rich ds DNA/Cu NPs-based fluorescence biosensing platform is investigated by using target NF-κB p50 under gradient concentrations (Figure 3A). Figure 3B illustrates the relationship between the NF-κB p50 concentration and the fluorescence intensity at the maximum emission wavelength (588 nm). In the concentration range from 0.1 to 5 pM, the fluorescence intensity exhibits a linear correlation to NF-κB p50 concentration (inset of Figure 3B). According to the rule of three times standard deviation of the response over the slope of the calibration curve, the detection limit is estimated to be 0.096 pM, which is comparable to that of the previously reported methods. Table S2 compares the performance of the developed biosensors to some previous fluorescent, electrochemical, and colorimetric assay for sensing NF-κB p50. Briefly, the sensitivity of the proposed assay has improved by 400-fold as compared with label-free biosensor-based electrochemical assay (40 pM) (Chen et al., 2014), 40-fold as compared with isothermal exponential amplification-based colorimetric assay (3.8 pM) (Zhang et al., 2012), 10-fold as compared with target-converted helicase-dependent amplification-based fluorescent assay (0.93

pM) (Cao et al., 2013), and is comparable to the near-infrared solid-phase rolling circle amplification-based fluorescent assay (0.14 pM) but with a more simple procedure (Yin et al., 2014). Such significant improvement in the detection sensitivity might attribute to the combination of hairpin DNA cascade reaction for signal amplification.

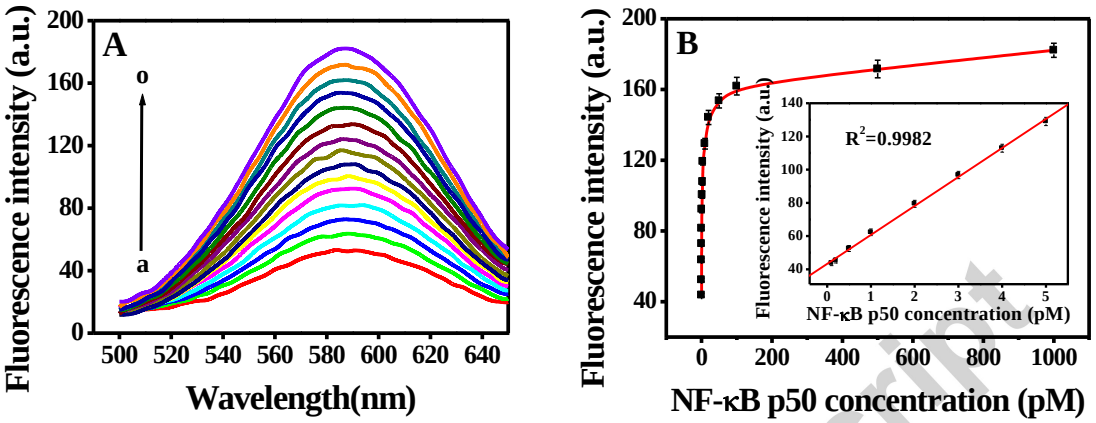

Figure 3. (A) Fluorescence response corresponding to the analysis of NF-κB p50 at different concentrations: (a) 0, (b) 0.1, (c) 0.2, (d) 0.5, (e) 1, (f) 2, (g) 3, (h) 4, (i) 5, (j) 10, (k) 20, (l) 50, (m) 100, (n) 500, and (o) 1000 pM. (B) The relationship between the fluorescence intensity and NF-κB p50 concentration. Inset: the linear range between the fluorescence intensity and the concentrations of NF-κB p50 from 0.1 to 5 pM. The error bars were the standard deviation of three repetitive measurements.

3.5. Specificity, reproducibility and stability of AT-rich ds DNA/Cu NPs-based fluorescent biosensing platform for NF-κB p50 detection

Sensitivity and specificity are two key factors for a successful sensing system for protein detection. In this system, the sensitivity mainly depends on the efficiency of HDCA for signal amplification. The detection specificity is basically determined by specific recognition function for target NF-κB p50. To evaluate the detection specificity, we challenged the system with the target NF-κB p50 and several non-targeted proteins such as BSA, HSA, IgG and human thrombin. The results are shown in Figure 4. As can be seen, the specific target NF-κB p50 leads to a significant increase of fluorescence intensity. In contrast, no obvious variation of fluorescence intensity can be observed in the presence of other non-targeted proteins. Good specificity exhibited for the target NF-κB p50.

As for biosensors, not only the sensitivity and specificity but two other crucial factors, reproducibility and stability, should also be taken into account. The reproducibility and stability of the proposed sensing platform were investigated. Figure S5A shows that the relative standard derivation of 10 independent tests for NF-κB p50 is 2.36%. It verifies that the good reproducibility for sensing platform. Furthermore, the stability of the proposed sensing platform is shown in Figure S5B. The fluorescence response of the AT-rich ds DNA/Cu NPs-based biosensing platform for NF-κB p50 has little apparent change in the continuous seven days by everyday detection. Therefore, the results are accordant with our proposed sensing mechanism and clearly demonstrate that the developed sensing platform could offer high specificity, reproducibility and stability for ultra-sensitive detection of target NF-κB p50.

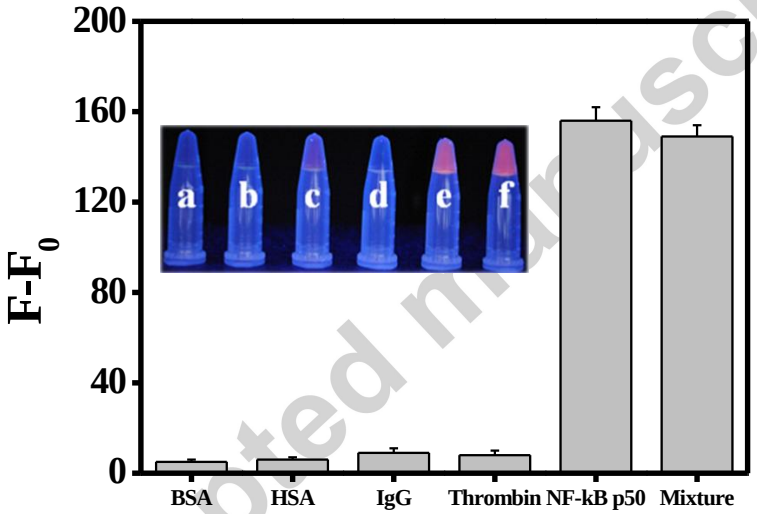

Figure 4. Fluorescence responses of AT-rich ds DNA/Cu NPs in the presence of 500 pM NF-κB p50 or 5 nM other analytes. The inset shows the corresponding fluorescent emission images with UV-light excitation: (a) BSA, (b) HSA, (c) IgG, (d) Thrombin, (e) NF-κB p50, (f) Mixture. The error bars were the standard deviation of three repetitive measurements.

3.6. Detection of NF-κB p50 in Hela cell nuclear extracts

Samples	Added (pM)	Found (pM)	Recovery (%)	RSD (%) n=3
1	1	1.05	105.00	6.76
2	5	4.98	99.60	7.25
3	10	10.15	101.50	4.85
4	50	50.56	101.12	5.54
5	100	98.56	98.56	6.36

Table 1. Results of the recovery test of NF-κB p50 in Hela cell nuclear extracts.

A big challenge for an excellent protein assay is the ability to be applied in biological sample. However, the proposed strategy does not involve any enzyme, the false positives caused by non-specific protein binding and the negative effect of the endogenous nuclease in the real samples could be eliminated. HeLa cell nuclear extracts samples were spiked with NF-κB p50 at five concentrations (1, 5, 10, 50, and 100 pM) and then analyzed. The experimental results are summarized in Table 1, which shows that recovery was in the range of 98.56–105.00% with the RSDs between 4.85% and 7.25% (n=3). All the results indicate a satisfactory application of the developed sensing platform and it has great potential to be applied to target NF-κB p50 detection in biological samples, such as HeLa cell nuclear extracts, and further for the treatment research of crucial diseases in biomedical fields.

4. Conclusions

In summary, we have demonstrated a label-free and enzyme-free transcription factors biosensor by combining AT-rich ds DNA/Cu NPs as fluorescent indicator and hairpin DNA cascade reaction as signal amplifier. The proposed strategy presents multifaceted advantages over currently available assays: (i) The use of ingenious triplex DNA structure coupled with hairpin DNA cascade amplifier provides a significant amplification of detection signal, which affords a high sensitivity for the fluorescent sensing platform. With the use of NF-κB p50 as a proof-of-concept analyte, this sensing platform can detect NF-κB p50 specifically with a detection limit as low as 0.096 pM. (ii) Compared with fluorescent-labelled TFs assay, the ds DNA/Cu NPs probes used in this research do not need labelling or modifying, so the construction of the biosensor is very easy, without any requirement for chemical modification and offers a convenient probe for analyte detection. (iii) The whole reaction performed in the isothermal solution without the requirement of troublesome and time-consuming thermal cycling, making the strategy extremely simple and cost-effective. The proposed biosensor uses a separation-free procedure where the assay conducted in a homogeneous solution. (iv) Furthermore, we have proven its capabilities to be applied in biological sample, demonstrating its potential for clinical use. (v) More importantly, this biosensor could be extended to sensitive detection of other DNA-binding proteins by simply changing corresponding recognition sequence of the probes. Therefore, we posit that the present label-free, enzyme-free, simple and cost-effective fluorescent biosensor has great potential to be used as a universal tool for ultra-sensitive analysis of NF-κB p50 or other proteins and may find wide applications in clinical diagnosis and biomedical fields.

Acknowledgements

This work is financially supported by the Projects (21073001, 21005001 and 21371007) from National Natural Science Foundation of China, Natural Science Foundation of Anhui (1608085MB46) the project of Anhui Key Laboratory of Controllable Chemistry Reaction & Material Chemical Engineering (OFCC0905) and Anhui Normal University Undergraduate Training Programs for Innovation and Entrepreneurship (201310370047).

References

Altevogt, D., Hrenn, A., Kern, C., Clima L., Bannwartha, W., Merfort, I., 2009. Org. Biomol. Chem. 7, 3934–3939.

Barany, F., 1991. Proc. Natl. Acad. Sci. U. S. A. 88, 189–193.

Cao, A., Zhang, C., 2013. Anal. Chem. 85, 2543−2547.

Chen, C., Wang, C., Jong, Y., Wu, S., 2015. Anal. Chem. 87, 6228−6232.

Chen, J.H., Zhang, X., Cai, S., Wu, D., Lin, J., Li, C., Zhang, J., 2014. Biosens. Bioelectron. 53, 12–17.

Chen, J., Liu, J., Fang, Z., Zeng, L., 2012. Chem. Commun. 48, 1057–1059.

Clark, K.L., Yutzey, K.E., Benson, D.W., 2006. Annu. Rev. Physiol. 68, 97−121.

Darnell, J.E., Jr., 2002. Nat. Rev. Cancer. 2, 740−749.

Dirks, R.M., Pierce, N.A., 2004. Proc. Natl. Acad. Sci. U. S. A. 101, 15275–15278.

Eggert, M., Kluter, A., Zettl, U.K., Neeck, G., 2004. Curr. Pharm. Des. 10, 2787−2796.

Enkin, N., Wang, F., Sharon, E., Bauke Albada, H., Willner, I., 2014. ACS Nano. 8, 11666–11673.

Fire, A., Xu, X., 1995. Proc. Natl. Acad. Sci. U. S. A. 92, 4641–4645.

Guo, Y., Wu, J., Ju, H., 2015. Chem. Sci. 6, 4318–4323.

Ihara, T., Ishii, T., Araki, N., Wilson, A.W., Jyo, A., 2009. J. Am. Chem. Soc. 131, 3826–3827.

Kennedy, T.A.C., MacLean, J.L., Liu, J., 2012. Chem. Commun. 48, 6845−6847.

Koval, I.A., Gamez, P., Belle, C., Selmeczi, K., Reedijk, J., 2006. Chem. Soc. Rev. 35, 814−840.

Li, B., Ellington, A.D., Chen, X., 2011. Nucleic Acids Res. 39, e110.

Li, C., Qiu, X., Hou, Z., Deng, K., 2015. Biosens. Bioelectron. 64, 505–510.

Li, J., Fu, H., Wu, L., Zheng, A., Chen, G., Yang, H., 2012. Anal. Chem. 84, 5309−5315.

Liu, X., Ouyang, L., Cai, X., Huang, Y., Feng, X., Fan, Q., Huang, W., 2013. Biosens. Bioelectron. 41, 218–224

McCann, J., Ames, B.N., 1976. Proc. Natl. Acad. Sci. U. S. A. 73, 950–954.

McCann, J., Choi, E., Yamasaki, E., Ames, B.N., 1975. Proc. Natl. Acad. Sci. U. S. A. 72, 5135–5139.

Monson, C.F., Woolley, A.T., 2003. Nano Lett. 3, 359−363.

Pabo, C.O., Sauer, R.T., 1992. Annu. Rev. Biochem. 61, 1053−1095.

Peng, S.L., 2008. Front. Biosci. 13, 4218−4240.

Quan, K., Huang, J., Yang, X., Yang, Y., Ying, L., Wang, H., He, Y., Wang, K., 2015. Chem. Commun. 51, 937–940.

Qing, T., Qing, Z., Mao, Z., He, X., Xu, F., Wen, L., He, D., Shi, H., Wang, K., 2014. RSC Adv. 4, 61092–61095.

Qing, Z., He, X., He, D., Wang, K., Xu, F., Qing, T., Yang, X., 2013a. Angew. Chem. Int. Ed. 52, 9719−9722.

Qing, Z.H., He, X.X., Qing, T.P., Wang, K.M., Shi, H., He, D.G., Zou, Z., Yan, L., Xu, F.Z., Ye, X.S., Mao, Z.G., 2013b. Anal. Chem. 85, 12138–12143.

Qing, Z., Mao, Z., Qing, T., He, X., Zou, Z., He, D., Shi, H., Huang, J., Liu, J., Wang, K., 2014. Anal. Chem. 86, 11263−11268.

Richards, C.I., Choi, S., Hsiang, J.C., Antoku, Y., Vosch, T., Bongiorno, A., Tzeng, Y.L., Dickson, R.M., 2008. J. Am. Chem. Soc. 130, 5038−5039.

Rotaru, A., Dutta, S., Jentzsch, E., Gothelf, E., Mokhir, A., 2010. Angew. Chem. Int. Ed. 49, 5665−5667.

Saiki, R.K., Gelfand, D.H., Stoffel, S., Scharf, S.J., Higuchi, R., Horn, G.T., Mullis, K.B., Erlish, H.A., 1988. Science. 239, 487–491.

Sanchez, A.P., Sharma, K., 2009. Expert Rev. Mol. Med. 11, e13.

Sapsford, K.E., Algar, W.R., Berti, L., Gemmill, K.B., Casey, B.J., Oh, E., Stewart, M.H., Medintz, I.L., 2013. Chem. Rev. 113, 1904−2074.

Sen, R., Baltimore, D., 1986. Cell. 47, 921−928.

Song, Q., Shi, Y., He, D., Xu, S., Ouyang, J., 2015. Chem. Eur. J. 21, 2417–2422.

Spitz, F., Furlong, E.E., 2012. Nat. Rev. Genet. 13, 613−626.

Tang, Y., Lin, Y., Yang, X., Wang, Z., Chris Le, X., Li, Feng., 2015. Anal. Chem. 87, 8063−8066.

Tan, Y.N., Su, X., Zhu, Y., Lee, J.Y., 2010. ACS Nano. 4, 5101–5110.

Teng, Y., Jia, X., Li, J., Wang E., 2015. Anal. Chem. 87, 4897−4902.

Xiao, Z., Guo, X., Ling, L., 2013. Chem. Commun. 49, 3573–3575.

Xu, J., Gao, Y., Li, B., Jin, Y., 2015. Biosens. Bioelectron. 80, 91–97.

Walker, G.T., Fraiser, M.S., Schram, J.L., Little, M.C., Nadeau, J.G., Malinowski, D.P., 1992. Nucleic Acids Res. 20, 1691–1693.

Wang, H.B., Zhang, H.D., Chen, Y., Liu, Y.M., 2015. Biosens. Bioelectron. 74, 581–586.

Wu, C., Cansiz, S., Zhang, L., Teng, I., Qiu, L., Li, J., Liu, Y., Zhou, C., Hu, R., Zhang, T., Cui, C., Cui, L., Tan, W., 2015. J. Am. Chem. Soc. 137, 4900−4903.

Yin, B.C., Ye, B.C., Tan, W., Wang, H., Xie, C., 2009. J. Am. Chem. Soc. 131, 14624−14625.

Yin, J., Gan, P., Zhou, F., Wang, J., 2014. Anal. Chem. 86, 2572−2579.

Yin, P., Choi, H.M.T., Calvert, C.R., Pierce, N.A., 2008. Nature. 451, 318–323.

Zhang, Y., Hu, J., Zhang, C., 2012. Anal. Chem. 84, 9544−9549.

Zhang, L., Cai, Q.Y., Li, J., Ge, J., Wang, J.Y., Dong, Z.Z., Li, Z.H., 2015a. Biosens. Bioelectron. 69, 77–82.

Zhang, Y., Yan, Y., Chen, W., Cheng W., Li, S., Ding, X., Li, D., Wang, H., Ju, H., Ding, S., 2015b. Biosens. Bioelectron. 68, 343–349.

Highlight

• A label-free, enzyme-free, ultrasensitive TFs biosensor was constructed.

• AT-rich dsDNA/Cu NPs was used as the signal in the assay.

• Hairpin DNA cascade reaction amplification (HDCA) was employed in the biosensor.

• It is a separation-free procedure conducted in a homogeneous solution